Synthesis and Characterization of Multiresponsive Core−Shell Microgels

Clinton D. Jones and L. Andrew Lyon*

School of Chemistry and Biochemistry, Georgia Institute of Technology, Atlanta, Georgia 30332-0400

Received August 8, 2000; Revised Manuscript Received September 8, 2000

ABSTRACT: We report the synthesis and characterization of temperature and pH responsive hydrogel particles (microgels) with core−shell morphologies. Core particles composed of cross-linked poly(*N*-isopropylacrylamide) (*p*-NIPAm) or poly(NIPAm-*co*-acrylic acid) (*p*-NIPAm-AAc) were synthesized via precipitation polymerization and then used as nuclei for subsequent polymerization of *p*-NIPAm-AAc and *p*-NIPAm, respectively. The presence of a core−shell morphology was confirmed by transmission electron microscopy (TEM). Thermally initiated volume phase transitions were interrogated via temperature-programmed photon correlation spectroscopy (TP-PCS) as a function of solution pH. The *p*-NIPAm-AAc core hydrogel displays both a strong temperature and pH dependence on swelling. However, both *p*-NIPAm-AAc (core)/*p*-NIPAm (shell) and *p*-NIPAm (core)/*p*-NIPAm-AAc (shell) particles display a more complex pH dependence than the homogeneous particles. Specifically, a multistep volume phase transition appears when the AAc component becomes highly charged at a high pH. It is apparent from the measured deswelling curves that a portion of the particle swelling behavior is dominated by *p*-NIPAm, regardless of its location in the particle. However, deswelling behavior that is due to a mixture of *p*-NIPAm-AAc and *p*-NIPAm is evident, as well as a regime that is largely attributed to *p*-NIPAm-AAc alone. Small differences in the effect of pH on the two core−shell particles indicate that the influence of *p*-NIPAm is somewhat greater when it is localized in the shell.

Introduction

Microgels composed of environmentally responsive polymers continue to attract attention due to their potential applications in numerous fields,[1] including drug delivery,[2−5] chemical separations,[6−8] sensors,[9−12] and catalysis.[13,14] Perhaps the most widely studied class of responsive polymers are temperature responsive poly(alkylacrylamides), specifically poly(*N*-isopropylacrylamide).[1,15−17] Part of the appeal of these materials stems from the varied physical properties of *p*-NIPAm latices that are modulated by the phase transition, including hydrophobicity,[18] particle size,[19,20] porosity, refractive index, colloidal stability,[21] scattering cross section,[22,23] electrophoretic mobility,[24−26] and rheology.[27,28] Because of the versatility of these materials, there has also been a growing interest into responsive latices that possess a more advanced architecture and hence are multifunctional. Numerous responsive core−shell or core−corona particles have been synthesized either to introduce spatially localized chemical functionalities to the particle,[29−31] to impart thermoresponsivity to nonresponsive particles,[32] or to modify a specific physical property of the latex.[27,33,34]

Many of the core−shell particles described above contain both a responsive and nonresponsive component. However, there are many potential applications of multiresponsive core−shell particles that are composed of two or more environmentally sensitive polymers. Such materials present a potentially diverse chemo-mechanical system for study, as these particles would be expected to display very complex phase transition behavior. This is especially true in core−shell systems where one polymer has a chemical or mechanical influence over the swelling of the other polymeric component. In this paper, we present the synthesis and characterization of a multiresponsive (pH and temperature) core−shell hydrogel system that displays complex phase transition behavior. The effects of particle architecture and pH on the temperature-dependent swelling behavior are presented, as well as microscopic investigations into the resultant particle morphologies.

* To whom correspondence should be addressed: e-mail lyon@chemistry.gatech.edu.

Experimental Section

Materials. All reagents were purchased from Sigma-Aldrich. *N*-Isopropylacrylamide monomer (NIPAm) was recrystallized from hexanes (J.T. Baker) and dried in vacuo prior to use. Acrylic acid (AAc), *N*,*N*′-methylenebis(acrylamide) (BIS), sodium dodecyl sulfate (SDS), and ammonium persulfate (APS) were all used as received. Water for all reactions, solution preparation, and polymer purification was distilled, purified to a resistance of 18 MΩ (Barnstead E-Pure system), and filtered through a 0.2 μm filter to remove particulate matter.

Preparation of Core−Shell Hydrogel Nanoparticles. Hydrogel nanoparticles were prepared via aqueous free-radical, precipitation polymerization under a nitrogen atmosphere. A detailed description of this polymerization method may be found elsewhere.[1,35] All particles were purified via dialysis (Spectra/Por 7 dialysis membrane, MWCO 10 000, VWR) against frequent changes of stirring H_2O for 2 weeks at 5 °C.

Poly(NIPAm) Core. NIPAm (1.4 g) and BIS (0.10 g) were dissolved in 150 mL of H_2O and then filtered twice through a membrane filter (Pall Gelman Metricel). Dissolved gas was removed under vacuum for at least 15 min. SDS (0.057 g) was then dissolved in the monomer solution, which was filtered once again. H_2O (40 mL) was used to transfer and wash throughout filtration. The solution was placed into a 250 mL three-neck, round-bottom flask and heated over period of 1 h with a heating mantle under a constant nitrogen purge and maximum stir rate (Corning magnetic stirrer). After stabilizing for 15 min at 70 °C, polymerization was initiated via addition of APS (0.069 g) dissolved 10 mL of degassed H_2O. The reaction was allowed to proceed at a temperature of 70 °C for 6 h.

10.1021/ma001398m CCC: $19.00
Published on Web 10/12/2000

Poly(NIPAm-*co*-AAc) Shell. All random copolymers were prepared with a 9:1:0.5 ratio of comonomers (NIPAm:AAc:BIS). NIPAm (1.3 g), BIS (0.10 g), and AAc (0.072 g) were dissolved in 150 mL of H_2O and filtered in the same manner as above. SDS (0.057 g) and APS (0.069 g) were then added to the solution. H_2O (50 mL) was used to transfer and wash throughout filtration. After degassing under vacuum for 15 min, the solution was then purged with nitrogen for 1 h at room temperature. The *p*-NIPAm core solution (150 mL volume) was heated and maintained at 70 °C for 15 min at a maximum stir rate in a 500 mL three-neck, round-bottom flask, after which 30 mL of the NIPAm + AAc shell solution was added. After reacting for 30 min at 70 °C, the remaining 170 mL of shell solution was added in 10 mL aliquots via a syringe over a period of 45 min. The reaction was allowed to proceed at a temperature of 70 °C for 6 h.

Poly(NIPAm-*co*-AAc) Core. NIPAm (1.3 g), BIS (0.10 g), and AAc (0.072 g) were dissolved in 150 mL of H_2O. The amounts of surfactant and initiator were the same as for the *p*-NIPAm core above, as well as all other reaction conditions.

Poly(NIPAm) Shell. NIPAm (1.4 g) and BIS (0.10 g) were fully dissolved in 150 mL of H_2O. The amounts of surfactant and initiator were the same as for the *p*-NIPAm-AAc shell above, as well as all other reaction conditions.

Photon Correlation Spectroscopy. Particle sizes and polydispersities were determined via temperature-programmed photon correlation spectroscopy[36] (TP-PCS, Protein Solutions Inc.) as described previously.[37] A 0.01 M HCl stock solution was used for pH adjustment prior to measurement. In the data presented below, each point corresponds to the average of 20 measurements, each having a 15 s integration time. The solution was allowed to equilibrate thermally for 10 min before each set of measurements. Particle sizes were obtained by fitting the collected correlelograms to a distribution of diffusion coefficients.[37] These values were then converted to a range of particle sizes via the Stokes−Einstein relationship. Data fitting was accomplished with a proprietary regularization algorithm that accounts for multimodal populations and non-Gaussian distributions (DYNALS, Protein Solutions).

TEM. To visualize the core−shell structure of the particles, the AAc groups were selectively stained with uranyl acetate (Polysciences). Particles were stained by mixing 0.050 mL of dialyzed particle solution with 0.5 mL of 0.75 mM uranyl acetate and agitated for 1 h. A Formvar-coated Cu TEM grid (Ted Pella) was placed onto a Kimwipe, and one drop of the stained particle solution was applied. The grid was then dried overnight at ambient temperature. TEM images were acquired with a JEOL 100CX II (120 kV).

Results and Discussion

Both the core and core−shell particles presented here were prepared by precipitation polymerization at 70 °C in aqueous media. This is a convenient method for preparing *p*-NIPAm particles, as the monomer is readily soluble under the reaction conditions, but the polymer undergoes a phase separation into dense polymer globules.[15,16,35] In the synthesis of the shell polymer, the collapsed particles serve as nuclei for further polymerization, thereby resulting in preferential growth of the existing particles over the nucleation of new ones. The results of this method can be seen in the TEM images shown in Figure 1; staining of the AAc groups by uranyl acetate allows for easy visualization of the core−shell structure. These images also suggest that the interface between the two materials is fairly sharp and not highly interpenetrated. Given our method of particle synthesis, this result is expected; shell polymerization inside the core particles is sterically hindered due to the high density of the globular core at 70 °C. It should be noted that the particle size measured by this technique is somewhat unreliable as the particles may have a tendency to flatten and spread on the TEM grid during the sample preparation. This can also lead to a larger apparent polydispersity; individual particles are not expected to interact with the substrate in a homogeneous fashion. It is for these reasons that we perform particle sizing via the less perturbing method of photon correlation spectroscopy.

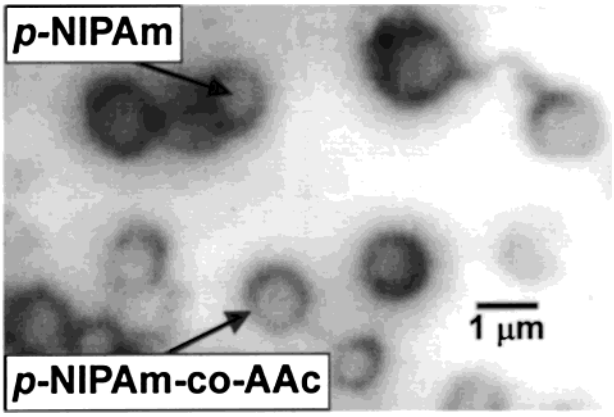

Figure 1. Transmission electron micrograph of *p*-NIPAm (core)/*p*-NIPAm-*co*-AAc (shell) hydrogel particles. The AAc component of the particles was preferentially stained with uranyl acetate in order to visualize the core−shell structure of the particles.

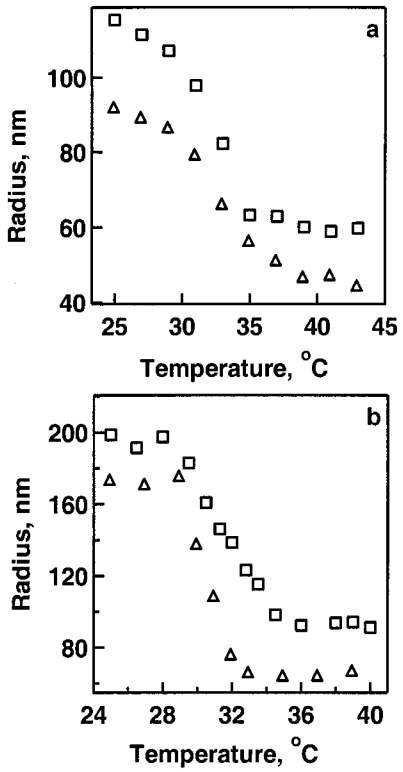

Figure 2. Core and core−shell deswelling curves obtained at pH 3.5: (a) *p*-NIPAm core before (Δ) and after (□) addition of a *p*-NIPAm-AAc shell; (b) *p*-NIPAm-AAc core before (Δ) and after (□) addition of a *p*-NIPAm shell. For both sets of curves, the noticeable size increase at all temperatures indicates the addition of shell to the preexisting core particles.

TP-PCS data for two typical core−shell particle preparations are shown in Figure 2. Figure 2a shows the phase transition at pH 3.5 for a 5% cross-linked (BIS) *p*-NIPAm particle before (Δ) and after (□) addition of a 5% cross-linked *p*-NIPAm-AAc shell. Increases in particle size both above and below the lower critical solution temperature (LCST) indicate that polymer has

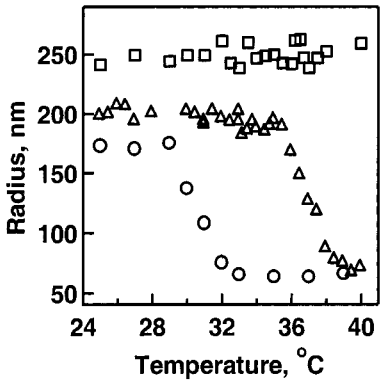

Figure 3. Deswelling curves for *p*-NIPAm-AAc particles at pH 3.5 (○), 4.5 (Δ), and 6.5 (□). Both the particle size and LCST increase as the amount of AAc deprotonation is increased.

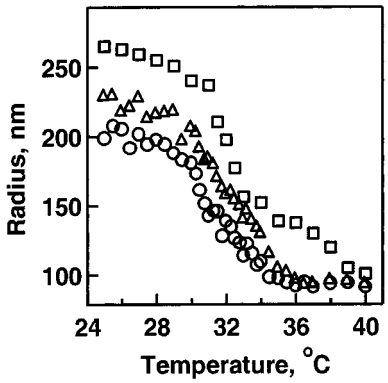

Figure 4. Deswelling curves for *p*-NIPAm-AAc (core)/*p*-NIPAm (shell) particles at pH 3.5 (○), 4.5 (Δ), and 6.5 (□). Only slight differences are noticeable between pH 3.5 and 4.5, both of which appear to be very similar to curves obtained for *p*-NIPAm alone. The pH 6.5 curve, however, displays two phase transitions at 32 and 38 °C, reflecting a degree of heterogeneity in the individual particles and a strong modulation of the *p*-NIPAm-AAc transition by *p*-NIPAm.

indeed been added to the particles, as supported by the TEM data. Calculated polydispersities (from PCS fits) were between 15% and 20% for all batches of particles at all temperatures, indicating that the nucleation of new particles during shell synthesis is negligible. Furthermore, we see no evidence of non-(core/shell) particles in our TEM images. Similar results are obtained when *p*-NIPAm-AAc particles are used as the core and a shell of *p*-NIPAm is added (Figure 2b). It should be noted that small shifts in the LCST are observed upon addition of shell in both cases. When *p*-NIPAm-AAc is added to *p*-NIPAm, the LCST shifts to lower temperatures and sharpens slightly, as is characteristic of NIPAm-AAc copolymers.[15,16] Likewise, following addition of *p*-NIPAm to a *p*-NIPAm-AAc core, the deswelling curve shows an LCST shift to higher temperatures and a small degree of curve broadening. While these effects are subtle, they suggest that the observed core−shell swelling properties are different from those of the core particles alone.

As stated above, *p*-NIPAm-AAc can be considered to be a multiresponsive polymer due to its sensitivity to both temperature and pH. This effect is illustrated by the pH-dependent swelling behavior of the *p*-NIPAm-AAc core particles (Figure 3). At pH 3.5 (○), where the majority of AAc groups are protonated, the LCST is observed at ∼30 °C. When the AAc groups are partially deprotonated (pH 4.5, Δ), the average particle size increases and the LCST shifts to ∼36 °C. This effect has been explained as being due to both an increased osmotic pressure resulting from counterion ingress and chain−chain Coulombic repulsion resulting in an increase in the average interchain distance.[26,38] A more dramatic manifestation of this is evident at pH 6.5 (□), where the particle size increases further and no LCST is evident in the monitored temperature window. Previous studies on similar particles have shown that an LCST occurs at ∼60 °C under these conditions.[38] At this pH, a majority of the AAc is deprotonated, thereby inhibiting particle collapse via a further increase in osmotic pressure and Coulombic repulsion.

Significantly different behavior is observed, however, when the *p*-NIPAm-AAc microgel is coated with *p*-NIPAm to form a *p*-NIPAm-AAc (core)/*p*-NIPAm (shell) particle. The data shown in Figure 4 suggest that the *p*-NIPAm shell largely dominates the swelling behavior, even though it comprises only a small percentage of the total particle volume. In contrast to the core particle behavior, only a small shift in LCST is observed between pH 3.5 (○) and 4.5 (Δ). The *p*-NIPAm shell collapse transition apparently causes the *p*-NIPAm-AAc core to deswell at a temperature >4 °C below its characteristic LCST (shown in Figure 3, Δ). A more complex effect is observed at pH 6.5 (□), where a large degree of particle collapse is observed at approximately the same temperature as the pH 4.5 LCST, followed by a second transition at 38 °C. Despite the fact that the characteristic LCST of the *p*-NIPAm-AAc copolymer alone is ∼60 °C at pH 6.5, the core−shell structure is able to collapse completely below 40 °C. These data suggest that there are at least two distinct particle domains at this pH. The first transition is considered to be due to collapse of the *p*-NIPAm shell accompanied by partial collapse of the *p*-NIPAm-AAc core. The second transition is attributed to further collapse of the *p*-NIPAm-AAc core. The depression of the core LCST (from 60 to <40 °C) is attributed to a decrease in the average interchain distance via the *p*-NIPAm shell collapse. Interestingly, the magnitude of the pH-induced equilibrium swelling is also depressed upon addition of the *p*-NIPAm shell. In fact, the core−shell particle diameter at pH 6.5 is nearly the same as that of the core alone at the same pH, suggesting that addition of the shell physically restricts the maximum swollen volume of the core.

A somewhat different pH dependence is observed when *p*-NIPAm-AAc is localized in the shell of the particle. In a fashion similar to the particles represented in Figure 4, the thermodynamics of the *p*-NIPAm (core)/*p*-NIPAm-AAc (shell) phase transition (Figure 5) deviate from those of a *p*-NIPAm-AAc core particle. The pH-induced LCST shifts observed for the *p*-NIPAm-AAc core (Figure 3) are diminished significantly; measured LCST values at pH 3.5 (○) and 4.5 (Δ) differ only slightly from one another, with the magnitude of the phase transition being similarly unperturbed. Furthermore, a phase transition is again observed for the core−shell particles upon raising the pH to 6.5 (□). However, the magnitude of the particle collapse is depressed in comparison to that of the *p*-NIPAm shell particles, and no second transition is evident in this temperature range. These data suggest that the pH-insensitive *p*-NIPAm core has a smaller overall influence over the collapse of *p*-NIPAm (core)/*p*-NIPAm-AAc (shell) particles than the inverse core−shell material. Furthermore, its control over the *magnitude* of the *p*-NIPAm-AAc swelling is also smaller than when *p*-NIPAm is present as the particle shell. These results are interpreted as an increased propensity

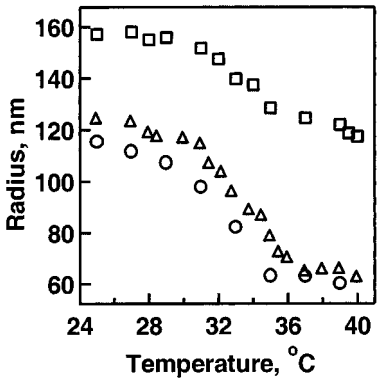

Figure 5. Deswelling curves for *p*-NIPAm (core)/*p*-NIPAm-AAc (shell) particles at pH (○), 4.5 (△), and 6.5 (□). Again, only slight differences are observable between the pH 3.5 and 4.5 curves. At pH 6.5, a small increase in LCST is observable, as is a decrease in the magnitude of the particle size change.

of the AAc component to swell when it is located in the particle shell; there is less physical restriction to pH-induced swelling in that architecture.

While the *p*-NIPAm component in both core−shell particles has an influence on the phase transition, at pH 6.5 there is still a large amount of excess swelling in the *p*-NIPAm (core)/*p*-NIPAm-AAc (shell) particles following the initial phase transition. To interrogate the complete deswelling behavior of the AAc component at high pH, TP-PCS was performed at temperatures up to 60 °C. Figure 6 shows the variation of particle size and swelling ratio over a large temperature range for both *p*-NIPAm (core)/*p*-NIPAm-AAc (shell) (○) and *p*-NIPAm-AAc (core)/*p*-NIPAm (shell) particles (△). As described above, the entire deswelling transition of the *p*-NIPAm-AAc (core)/*p*-NIPAm (shell) particles occurs below 40 °C, with the greatest volume change occurring at ∼32 °C. Conversely, only about 50% of the total *p*-NIPAm (core)/*p*-NIPAm-AAc (shell) particle collapse takes place below 40 °C. The remainder of the volume decrease can be divided into three distinct temperature regimes. A small but sharp transition is visible at 40 °C, followed by a broad, gradual volume decrease between 40 and 53 °C and finally a sharp transition at 54 °C. The greater complexity of these data reflect a

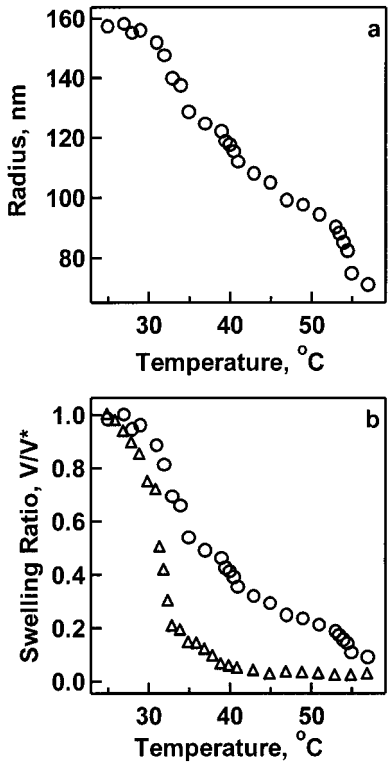

Figure 6. Wide temperature range deswelling behavior of *p*-NIPAm (core)/*p*-NIPAm-AAc (shell) (○) and *p*-NIPAm-AAc (core)/*p*-NIPAm (shell) (△) particles at pH 6.5. Panel a shows the change in particle radius with temperature, while panel b shows the same data plotted in terms of swelling ratio.

higher degree of structural heterogeneity when the higher LCST component is at the particle exterior. Unlike the case of the *p*-NIPAm-AAc (core)/*p*-NIPAm (shell) particle, where both the responsivity *and* the spatial boundaries of the high LCST polymer (i.e., deprotonated *p*-NIPAm-AAc) are restricted by *p*-NIPAm, in the inverted particle the outermost portion of the shell can swell largely unperturbed by *p*-NIPAm. Given this physical picture, we can qualitatively attribute the different regions of the *p*-NIPAm (core)/*p*-NIPAm-AAc (shell) deswelling curve (Figure 6b) to the following

Scheme 1. Temperature-Induced Deswelling of Core−Shell Hydrogel Nanoparticles

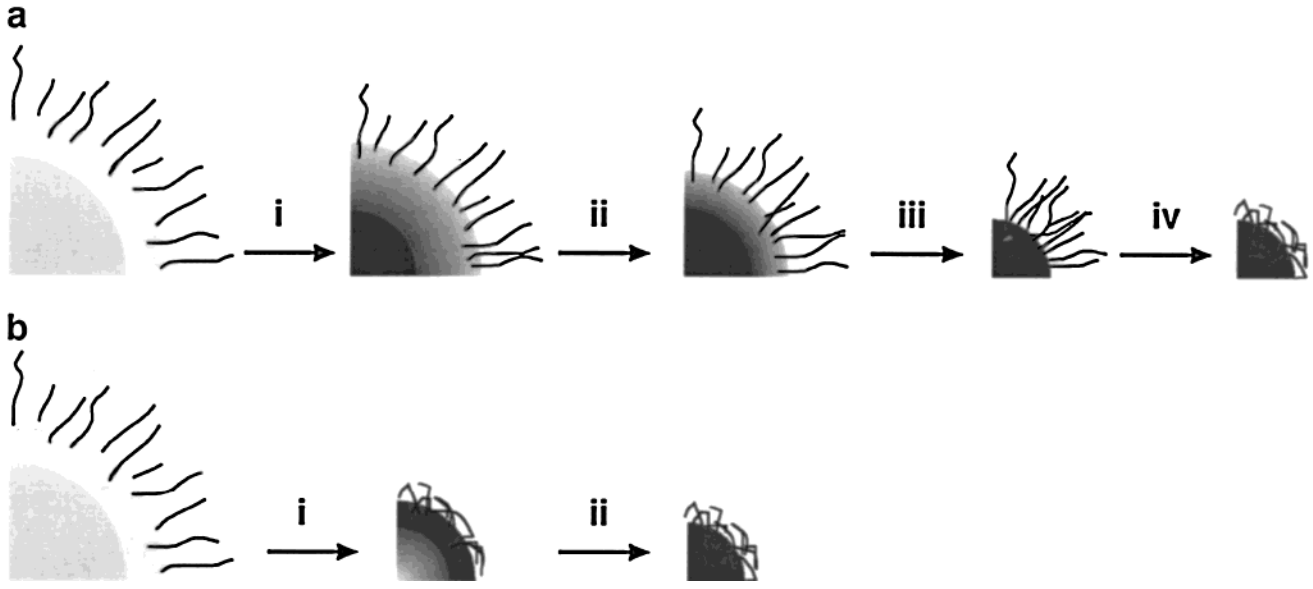

processes (illustrated in Scheme 1a): (i, 33 °C, transition) particle size decrease due to the *p*-NIPAm phase transition and physical interconnection of *p*-NIPAm and *p*-NIPAm-AAc at the core−shell interface, (ii, 40 °C, transition) collapse of the *p*-NIPAm-AAc component with a depressed LCST due to strong coupling to *p*-NIPAm, (iii, 40−53 °C, slow particle collapse) gradient of LCST values in the particle shell due to various degrees of coupling to the *p*-NIPAm core, and (iv, 54 °C, transition) collapse of the loosely cross-linked *p*-NIPAm-AAc shell exterior at a temperature that is characteristic of an unperturbed pH-sensitive microgel. The *p*-NIPAm-dominated collapse (i, 32 °C) and the perturbed *p*-NIPAm-AAc transition (ii, 38 °C) that occur in *p*-NIPAm-AAc (core)/*p*-NIPAm (shell) particles are illustrated in Scheme 1b. It should be noted that none of these transitions can be attributed to collapse of a subpopulation of non-(core/shell) particles, as the PCS-determined polydispersities of these colloidal sols do not increase at any temperature or at any pH. Regardless of the solution conditions or sample identity, the polydispersity is observed to be between 15% and 20%.

Our interpretations of these data are supported by previous studies showing that increases in external pressure can perturb *p*-NIPAm collapse and lower *p*-NIPAm-AAc hydrogel LCST values.[39,40] In our systems, the influence of *p*-NIPAm, whether present as a core or shell, can be thought of as changing the local pressure on the *p*-NIPAm-AAc, decreasing the interchain distance and thereby decreasing the LCST.[40] Furthermore, the *p*-NIPAm shell would be expected to produce a uniform and larger overall pressure, a hypothesis that is borne out by the greater influence of the *p*-NIPAm shell on the core−shell LCST values. The interpretation of region iv in Scheme 1a is also supported by previous studies, which have shown a radial gradient of cross-linker density in microgels, with the lowest density at the particle exterior.[41] It is therefore reasonable to assume that a similar gradient would be present in a shell prepared via precipitation polymerization. As a result, the shell exterior will be very weakly coupled to the swelling of the particle core and will display LCST behavior that does not deviate strongly from that of a homogeneous microgel or dilute solution of that polymer. Further investigations into the influence of cross-linker density and length on the coupling of core−shell phase transitions are currently underway.

Conclusions

The volume phase transition behavior of a new class of multiresponsive core−shell hydrogel nanoparticles has been interrogated by photon correlation spectroscopy. When two different responsive hydrogels, *p*-NIPAm (temperature responsive) and *p*-NIPAm-AAc (temperature and pH responsive), are arranged as the core and shell of a submicron-sized particle, the resultant environmental responsivity is strongly dependent on the respective location of the two materials. At pH 6.5, particles with a thin *p*-NIPAm shell surrounding a *p*-NIPAm-AAc core display two distinct volume phase transitions between 25 and 40 °C, corresponding to a *p*-NIPAm transition and a mixed *p*-NIPAm/*p*-NIPAm-AAc transition. However, when the arrangement of the two materials is reversed, *three* distinct volume phase transitions are observed between 25 and 60 °C, reflecting a more heterogeneous nanostructure in the submicron-sized hydrogel. This heterogeneity arises mainly from the fact that the expansion of the AAc-containing shell is subject to less physical restriction by *p*-NIPAm in this arrangement. Together, these results suggest that the core−shell architecture may be a powerful method for the construction of multiresponsive or multifunctional particles.

Acknowledgment. L.A.L. gratefully acknowledges financial support from Research Corporation in the form of a Research Innovation Award, from the National Science Foundation for a CAREER Award, and from the Arnold and Mabel Beckman Foundation for a Young Investigator Award. C.D.J. gratefully acknowledges financial support in the form of a Cherry-Emerson Fellowship from the Georgia Institute of Technology.

References and Notes

(1) Pelton, R. *Adv. Colloid Interface Sci.* **2000**, *85*, 1−33.
(2) Jeong, B.; Bae, Y. H.; Lee, D. S.; Kim, S. W. *Nature* **1997**, *388*, 860−862.
(3) Hoffman, A. "Intelligent" Polymers. In *Controlled Drug Delivery: Challenges and Strategies*; Park, K., Ed.; American Chemical Society: Washington, DC, 1997; pp 485−498.
(4) Kurisawa, M.; Terano, M.; Yui, N. *Macromol. Rapid Commun.* **1995**, *16*, 663−666.
(5) Brondsted, H.; Kopecek, J. *Pharm. Res.* **1992**, *9*, 1540−1545.
(6) Kawaguchi, H.; Fujimoto, K. *Bioseparation* **1998**, *7*, 253−258.
(7) Kayaman, N.; Kazan, D.; Erarslan, A.; Okay, O.; Baysal, B. M. *J. Appl. Polym. Sci.* **1998**, *67*, 805−814.
(8) Umeno, D.; Kawasaki, M.; Maeda, M. *Bioconjugate Chem.* **1998**, *9*, 719−724.
(9) Miyata, T.; Asami, N.; Uragami, T. *Macromolecules* **1999**, *32*, 2082−2084.
(10) Holtz, J. H.; Holtz, J. S. W.; Munro, C. H.; Asher, S. A. *Anal. Chem.* **1998**, *70*, 780−791.
(11) Holtz, J. H.; Asher, S. A. *Nature* **1997**, *389*, 829−832.
(12) Ouali, L.; Stoll, S.; Pefferkorn, E.; Elaissari, A.; Lanet, V.; Pichot, C.; Mandrand, B. *Polym. Adv. Technol.* **1995**, *6*, 541−546.
(13) Bergbreiter, D. E.; Case, B. L.; Liu, Y.-S.; Caraway, J. W. *Macromolecules* **1998**, *31*, 6053−6062.
(14) Nagayama, H.; Maeda, Y.; Shimasaki, C.; Kitano, H. *Macromol. Chem. Phys.* **1995**, *196*, 611−620.
(15) Shibayama, M.; Tanaka, T. Volume Phase Transition and Related Phenomena of Polymer Gels. In *Advances in Polymer Science*; Springer-Verlag: Berlin, 1993; Vol. 109, pp 1−62.
(16) Tanaka, T.; Fillmore, D. J.; Sun, S.-T.; Nishio, I.; Swislow, G.; Shah, A. *Phys. Rev. Lett.* **1980**, *45*, 1636−1639.
(17) Dowding, P. J.; Vincent, B.; Williams, E. *J. Colloid Interface Sci.* **2000**, *221*, 268−272.
(18) Kawaguchi, H.; Fujimoto, K.; Mizuhara, Y. *Colloid Polym. Sci.* **1992**, *270*, 53−57.
(19) Saunders, B. R.; Vincent, B. *J. Chem. Soc., Faraday Trans.* **1996**, *92*, 3385−3389.
(20) Saunders, B. R.; Crowther, H. M.; Morris, G. E.; Mears, S. J.; Cosgrove, T.; Vincent, B. *Colloid Surf. A: Physicochem. Eng. Asp.* **1999**, *149*, 57−64.
(21) Snowden, M. J.; Vincent, B. **1993**, *532*, 153−160.
(22) Yi, Y. D.; Oh, K. S.; Bae, Y. C. *Polymer* **1997**, *38*, 3471−3476.
(23) Yi, Y. D.; Bae, Y. C. *J. Appl. Polym. Sci.* **1998**, *67*, 2087−2092.
(24) Rasmusson, M.; Vincent, B.; Marston, N. *Colloid Polym. Sci.* **2000**, *278*, 253−258.
(25) Fernandez-Nieves, A.; Fernandez-Barbero, A.; de las Nieves, F. J.; Vincent, B. *J. Phys.: Condens. Matter* **2000**, *12*, 3605−3614.
(26) Fernandez-Nieves, A.; Fernandez-Barbero, A.; Vincent, B.; de las Nieves, F. J. *Macromolecules* **2000**, *33*, 2114−2118.
(27) Senff, H.; Richtering, W.; Norhausen, C.; Weiss, A.; Ballauff, M. *Langmuir* **1999**, *15*, 102−106.
(28) Senff, H.; Richtering, W. *J. Chem. Phys.* **1999**, *111*, 1705−1711.
(29) Duracher, D.; Sauzedde, F.; Elaissari, A.; Pichot, C.; Nabzar, L. *Colloid Polym. Sci.* **1998**, *276*, 920−929.
(30) Duracher, D.; Sauzedde, F.; Elaissari, A.; Perrin, A.; Pichot, C. *Colloid Polym. Sci.* **1998**, *276*, 219−231.

(31) Zhou, G.; Elaissari, A.; Delair, T.; Pichot, C. *Colloid Polym. Sci.* **1998**, *276*, 1131−1139.
(32) Matsuoka, H.; Fujimoto, K.; Kawaguchi, H. *Polym. J.* **1999**, *31*, 1139−1144.
(33) Kato, T.; Fujimoto, K.; Kawaguchi, H. *Polym. Gels Networks* **1994**, *2*, 307−313.
(34) Hazot, P.; Pichot, C.; Maazouz, A. *Macromol. Chem. Phys.* **2000**, *201*, 632−641.
(35) Wu, X.; Pelton, R. H.; Hamielec, A. E.; Woods, D. R.; McPhee, W. *Colloid Polym. Sci.* **1994**, *272*, 467−477.
(36) Pecora, R. *Dynamic Light Scattering*; Plenum Press: New York, 1985.
(37) Debord, J. D.; Lyon, L. A. *J. Phys. Chem. B* **2000**, *104*, 6327−6331.
(38) Ito, S.; Ogawa, K.; Suzuki, H.; Wang, B.; Yoshida, R.; Kokufuta, E. *Langmuir* **1999**, *15*, 4289−4294.
(39) Kato, E. *J. Chem. Phys.* **1997**, *106*, 3792−3797.
(40) Yamazaki, Y.; Tada, T.; Kunugi, S. *Colloid Polym. Sci.* **2000**, *278*, 80−83.
(41) Guillermo, A.; Addad, J. P. C.; Bazile, J. P.; Duracher, D.; Elaissari, A.; Pichot, C. *J. Polym. Sci., Part B: Polym. Phys.* **2000**, *38*, 889−898.

MA001398M